Hindawi Publishing Corporation
Journal of Nanomaterials
Volume 2015, Article ID 854310, 7 pages
http://dx.doi.org/10.1155/2015/854310

Research Article

Catalytic Activity of Co_3O_4 Nanomaterials with Different Morphologies for the Thermal Decomposition of Ammonium Perchlorate

Li-Na Jin,[1] Jian-Guo Wang,[1] Xin-Ye Qian,[1] Dan Xia,[2] and Ming-Dong Dong[2]

[1]*Institute for Advanced Materials and School of Materials Science and Engineering, Jiangsu University, Zhenjiang 212013, China*
[2]*Center for DNA Nanotechnology (CDNA), Interdisciplinary Nanoscience Center (iNANO), Aarhus University, 8000 Aarhus, Denmark*

Correspondence should be addressed to Li-Na Jin; jinln@mail.ujs.edu.cn and Ming-Dong Dong; dong@inano.au.dk

Received 9 March 2015; Accepted 20 April 2015

Academic Editor: P. Davide Cozzoli

Nano-Co_3O_4 with different morphologies was successfully synthesized by annealing $CoC_2O_4{\cdot}2H_2O$ precursors. The as-obtained samples were characterized by powder X-ray diffraction (XRD), scanning electron microscopy (SEM), and low-temperature nitrogen adsorption-desorption. It was found that the volume ratio of N,N-dimethylformamide (DMF) and water played an important role in the formation of cobalt oxalate precursors with different morphologies. After calcination in air, cobalt oxalate precursors converted to Co_3O_4 nanomaterials while their original morphologies were maintained. The catalytic effect was investigated for nano-Co_3O_4 with different morphologies on the thermal decomposition of ammonium perchlorate (AP) by differential scanning calorimeter (DSC). The results indicated that all products showed excellent catalytic activity for thermal decomposition of AP and the Co_3O_4 nanorods with larger BET surface area and pore volume had the highest catalytic activity.

1. Introduction

Morphology-controlled synthesis of inorganic nanomaterials is of extensive research interest in materials science because the electronic, optical, magnetic, and catalytic properties of nanocrystals are highly dependent on not only their composition, but also their structure [1], shape [2], and size [3]. Therefore, many efforts have been made to develop cost-effective synthesis methods of nanomaterials with different structures and morphologies for enabling novel intrinsic properties and applications of nanomaterials.

Co_3O_4, as one of the most intriguing magnetic p-type semiconductors, is of special interest due to its potential applications in heterogeneous catalyst [4], lithium-ion battery [5], supercapacitor [6], gas sensor [7], and many other aspects [8]. Up to now, shape-controlled Co_3O_4 nanostructures have been prepared by various approaches, in which morphology-conserved transformation of precursors has proved to be a promising approach for the synthesis of Co_3O_4 nanostructures [9–12]. For example, Zhu et al. reported the shape-controlled synthesis of cobalt carbonate/hydroxide intermediates via a solvothermal method at 220°C for 18 h [9]. Hu et al. synthesized β-$Co(OH)_2$ nanosheet at 180°C for 12 h and $Co(CO_3)_{0.5}(OH)_{0.11}H_2O$ nanobelt at 140°C for 12 h via a solvothermal method [10]. Wang et al. prepared one-dimensional and layered parallel folding of cobalt oxalate nanostructures using N,N-dimethylacetamide (DMA) and dimethyl sulfoxide (DMSO) as solvents at ambient temperature [11]. In our past work, we prepared shape-controlled synthesis of Co_3O_4 nanostructures derived from coordination polymer precursors [12]. However, for some shape-controlled synthesis methods, special instruments, complicated processes, long reaction times, and relatively high temperatures are required. Therefore, it is important to design a simple, rapid, low-temperature, and low-cost synthesis route to synthesize morphology-controlled cobalt precursors.

Over the past decades, ammonium perchlorate (AP) has received considerable attention because AP is an important

oxidizer in solid composite propellants for solid fueled rockets and the combustion behavior of propellants is highly relevant to the thermal decomposition of AP. The lower the temperature at which AP begins to decompose, the higher the burning rate of propellants [13–15]. Recently, Co_3O_4 nanomaterials with various morphologies have been used as effective catalyst to accelerate thermal decomposition of AP [12, 16–19].

In the present work, we report morphology-controlled preparation of cobalt oxalate precursors from the reaction of cobalt(II) nitrate hexahydrate and oxalic acid under mild conditions. It was found that the volume ratio of N,N-dimethylformamide (DMF) and water played a crucial role in the formation of cobalt oxalate with different morphologies. After calcination in air, the as-prepared cobalt oxalate precursors subsequently converted to porous Co_3O_4 nanomaterials while their original morphologies had been well maintained. To study their potential applications, the as-prepared nano-Co_3O_4 with different morphologies had been applied in the thermal decomposition of AP, which exhibited good activity.

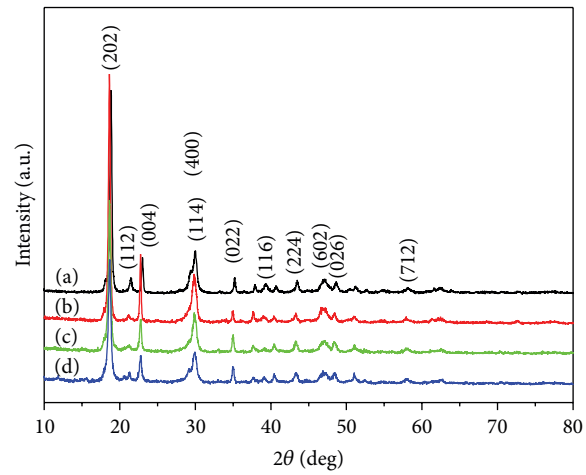

Figure 1: XRD patterns of the as-prepared precursors under the different volume ratio of DMF and water: (a) 0 : 20, (b) 4 : 16, (c) 8 : 12, and (d) 12 : 8.

2. Experimental

All chemicals and solvents are of analytical grade and were used as received without further purification. In a typical experiment, 1 mmol $Co(NO_3)_2{\cdot}6H_2O$ was dissolved in a mixed solution of DMF and deionized water at room temperature (the total volume is 20 mL), followed by addition of 1 mmol $H_2C_2O_4{\cdot}2H_2O$ under vigorous stirring. After 5 min, the as-obtained precipitates were centrifuged, washed with distilled water and absolute ethanol several times, and dried in vacuum at 60°C for 5 h. In addition, a calcination process (350°C for 1 h in air with a heating rate of 2°C min^{-1}) was performed to transform cobalt oxalate to black Co_3O_4 crystals. In the experiments, to obtain products with different morphologies, the volume ratio of DMF and water was adjusted while all other conditions were keeping unaltered.

The products were characterized by powder X-ray diffraction (XRD) on a Rigaku D/max 2500PC diffractometer with graphite monochromator and Cu K_α radiation (λ = 0.15406 nm) at a step width of 0.02°. SEM images of the products were obtained on scanning electron micro analyzers (HITACHI S-3400N,). Nitrogen adsorption-desorption isotherms, pore size distributions, and surface areas of the samples were measured by the instrument of NOVA 2000e using N_2 adsorption.

To test the catalytic effect of Co_3O_4 nanostructures with different morphologies on the thermal decomposition of AP, the mixture of AP and Co_3O_4 was ground carefully for 10 min and was detected by a differential scanning calorimeter (DSC) using STA 449C thermal analyzer with a heating rate of 10°C min^{-1} in N_2 atmosphere over the temperature range of 30–500°C. The mass percentage of Co_3O_4 nanostructures to AP in the mixture was 2%.

3. Results and Discussion

Figure 1 shows the XRD patterns of the precursors prepared under the different volume ratio of DMF and water. All of the diffraction peaks in Figure 1(a), 1(b), 1(c), and 1(d) can be indexed as the orthorhombic phase of $CoC_2O_4{\cdot}2H_2O$ by comparison with the data of JCPDS card files number 25-0250. No impurity peaks are detected in the XRD pattern.

Morphologies of all the precursors were characterized by SEM and the images of the samples are shown in Figure 2. When 20 mL of H_2O was used without addition of DMF, the result shown in Figure 2(a) reveals that sample is composed of $CoC_2O_4{\cdot}2H_2O$ microrods with diameter of about 2–5 μm. When 16 mL of H_2O and 4 mL of DMF were used, spindle-like $CoC_2O_4{\cdot}2H_2O$ nanostructures were obtained, shown in Figure 2(b). Figure 2(c) shows the morphology of sample prepared in the presence of 12 mL of H_2O and 8 mL of DMF. It was observed that the sample consisted of nanorod bundles. Figure 2(d) illustrates nanorods in sample prepared by using 8 mL of H_2O and 12 mL of DMF. In addition, when 4 mL of H_2O and 16 mL of DMF were used or 20 mL of DMF was used without addition of H_2O, no products could be obtained. The above facts showed that DMF/water volume ratio played an important role in the information of $CoC_2O_4{\cdot}2H_2O$. According to the previously reported studies, when only water was used as solvent, $CoC_2O_4{\cdot}2H_2O$ microrods were obtained because the ion-exchange reaction between the cobalt ion and the oxalate ion was very rapid in aqueous solution. In organic solvent medium, oxalic acid is a weak electrolyte that cannot be electrolytically dissociated into ions, so the cobalt ion and the oxalic acid do not react immediately. Therefore, when DMF and water were used, the reaction rate slowed down leading to smaller products, including spindle-like architectures, nanorod bundles, and nanorods. Furthermore, when the amount of DMF was increased to 16 mL or 20 mL, no products were obtained because the ion-exchange reaction was restrained [11].

The thermal behavior of $CoC_2O_4{\cdot}2H_2O$ microrods was investigated by thermogravimetric analysis (TGA) in static air atmosphere. From Figure 3, it can be seen that there are two distinct weight loss steps. The first weight loss

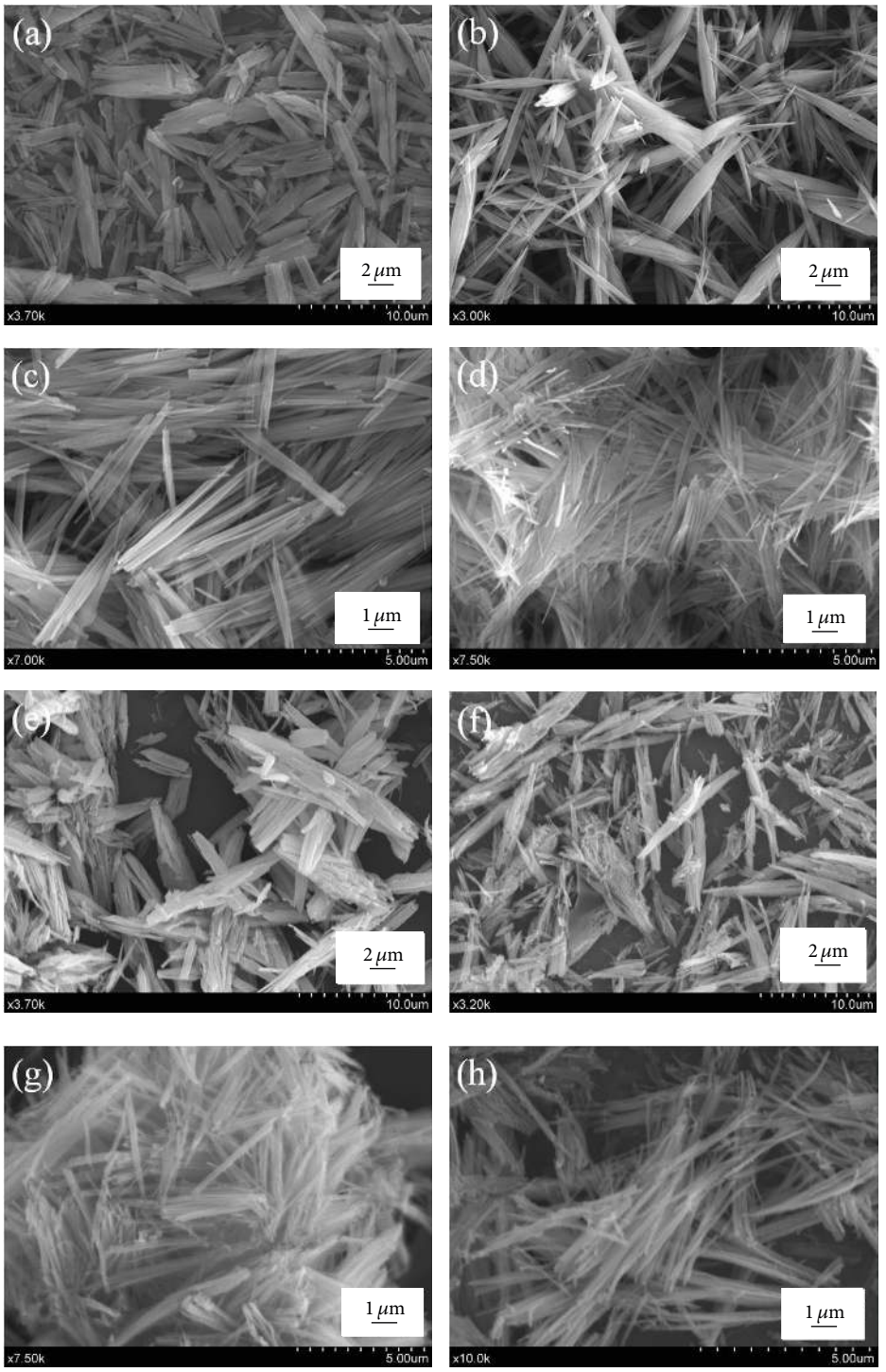

FIGURE 2: SEM images of the as-prepared cobalt oxalate precursors and Co_3O_4 nanostructures: (a, e) microrods, (b, f) spindle-like architectures, (c, g) nanorod bundles, and (d, h) nanorods.

occurs at 110–220°C, which corresponds to the evaporation of crystallized water. When the temperature is above 300°C, the second weight loss was observed, which is attributed to the decomposition of anhydrous oxalate into Co_3O_4. The weight loss of two steps is about 19.7% and 53.3%, which is close to the theoretical value. The decomposition of $CoC_2O_4 \cdot 2H_2O$ can be expressed as the following reaction:

$$\begin{aligned} CoC_2O_4 \cdot 2H_2O &\longrightarrow CoC_2O_4 + 2H_2O \uparrow \\ 3CoC_2O_4 + 2O_2 &\longrightarrow Co_3O_4 + 6CO_2 \uparrow \end{aligned} \quad (1)$$

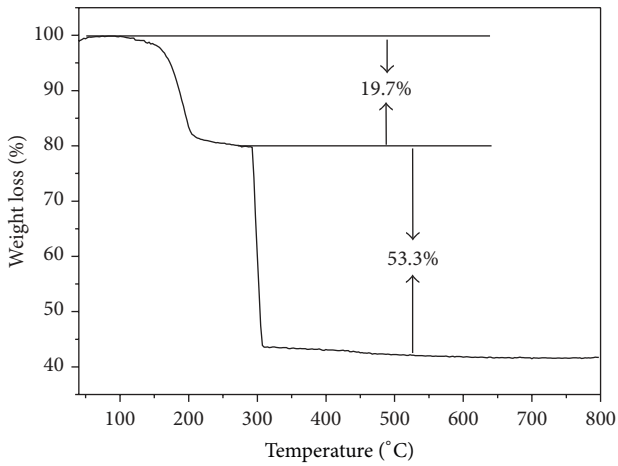

Figure 3: TGA curve of the as-obtained $CoC_2O_4{\cdot}2H_2O$ microrods.

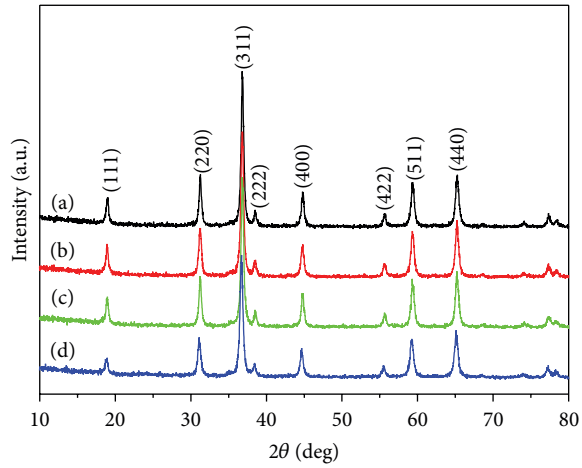

Figure 4: XRD patterns of the as-prepared Co_3O_4 nanostructures: (a) microrods, (b) spindle-like architectures, (c) nanorod bundles, and (d) nanorods.

According to the results of TGA, the thermal decomposition of the corresponding $CoC_2O_4{\cdot}2H_2O$ was performed at 350°C. After being annealed at 350°C for 1 h in air, the as-synthesized $CoC_2O_4{\cdot}2H_2O$ with different morphologies were completely converted to phase-pure spinel Co_3O_4. The morphology of the Co_3O_4 products is shown in Figures 2(e)–2(h), from which it can be seen that the original shape has been maintained after calcination. The crystallographic phase of all the samples is again examined by XRD (Figure 4). All diffraction peaks can be well indexed to the pure cubic phase of Co_3O_4 (JCPDS 43-1003), indicating that the pure phase of Co_3O_4 was obtained by annealing $CoC_2O_4{\cdot}2H_2O$ precursor directly. Figure 5 shows TEM images of the Co_3O_4 products, revealing that the Co_3O_4 products were composed of numerous Co_3O_4 nanoparticles with a size of several tens of nanometers and abundant pore structures were formed among the nanoparticles.

Nitrogen adsorption-desorption isotherms of nano-Co_3O_4 are shown in Figure 6, and the insets illustrate the corresponding Barrett-Joyner-Halenda (BJH) pore size distribution plots. The isotherms can be categorized as type IV with an H3 hysteresis loop, which is characteristic of mesoporous materials. The BJH pore size distribution indicates that all of the samples contain mesoscale pores. The Brunauer-Emmett-Teller (BET) surface areas and pore volumes of the samples are 42 m^2/g and 190.3 mm^3/g, 61 m^2/g and 226.3 mm^3/g, 62 m^2/g and 241.3 mm^3/g, and 83 m^2/g and 277.1 mm^3/g for the Co_3O_4 with microrods, spindle-like architectures, nanorod bundles, and nanorods, respectively.

Considering the porous structures and high BET surface area, we investigated the application of the synthesized nano-Co_3O_4 for the thermal decomposition of AP. Figure 7 shows DSC curves for thermal decomposition of pure AP and its mixture with nano-Co_3O_4 with different morphologies.

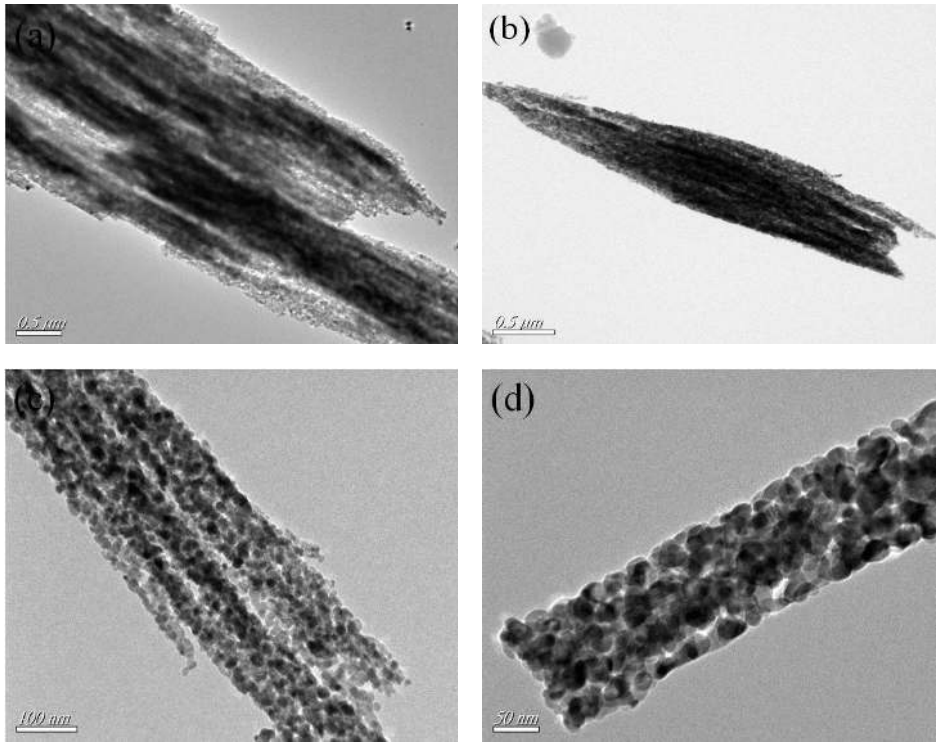

Figure 5: TEM images of the as-prepared Co_3O_4 nanostructures: (a) microrods, (b) spindle-like architectures, (c) nanorod bundles, and (d) nanorods.

For pure AP, an endothermic peak was observed at about 250°C, which is due to the crystal transformation of AP from orthorhombic to cubic phase (Figure 7(e)) [13]. When nano-Co_3O_4 with different morphologies as catalyst was added to AP, all samples have similar endothermic peaks at about 250°C, indicating that the catalysts have little effect on the crystallographic transition temperature of AP. However, in the relatively high temperature region, the samples containing catalysts have dramatic changes in the exothermic peaks of AP decomposition. When 2 wt% catalysts were added to AP, the original exothermic peak of pure AP at 445.0°C disappeared and only one exothermic peak was observed. The exothermic peak temperature was 305.1, 299.7, 297.4, and 296.2°C for Co_3O_4 microrods, spindle-like architectures, nanorod bundles, and nanorods, respectively (Figure 7(a)–7(d)). The present catalytic activity of Co_3O_4 nanorods was higher than Co_3O_4 nanoparticles, nanosheets, and octahedral particles [12, 18, 19]. The above results indicate that Co_3O_4 particles have a significant effect on the decomposition temperature of AP and Co_3O_4 nanomaterials with different morphologies for decreasing the decomposition of AP are proportional to their BET surface area and pore volume. It is known that specific surface area and pore volume can be the primary reasons for the catalytic role, since more reactive sites can be generated [12, 20, 21]. Thus, Co_3O_4 nanorods with larger BET surface area and pore volume have the most effective catalytic activity and the thermal decomposition temperature of AP shifted downward about 148.8°C.

4. Conclusions

In summary, we synthesized porous nano-Co_3O_4 with different morphologies via annealing $CoC_2O_4{\cdot}2H_2O$ precursors prepared under ambient condition without the assistance of template or surfactant. The as-prepared porous nano-Co_3O_4 with different morphologies have good catalytic properties for the thermal decomposition of AP due to their large BET surface area and pore volume. Co_3O_4 nanorods with larger BET surface area and pore volume show better catalytic activity than others and shifted the AP thermal decomposition temperature downwardly to about 148.8°C.

Conflict of Interests

The authors declare that there is no conflict of interests regarding the publication of this paper.

Acknowledgments

The authors acknowledge the financial support by National Natural Science Foundation of China (no. 21401081), China Postdoctoral Science Foundation (no. 2014M560397), Jiangsu Natural Science Funds for Distinguished Young Scholars

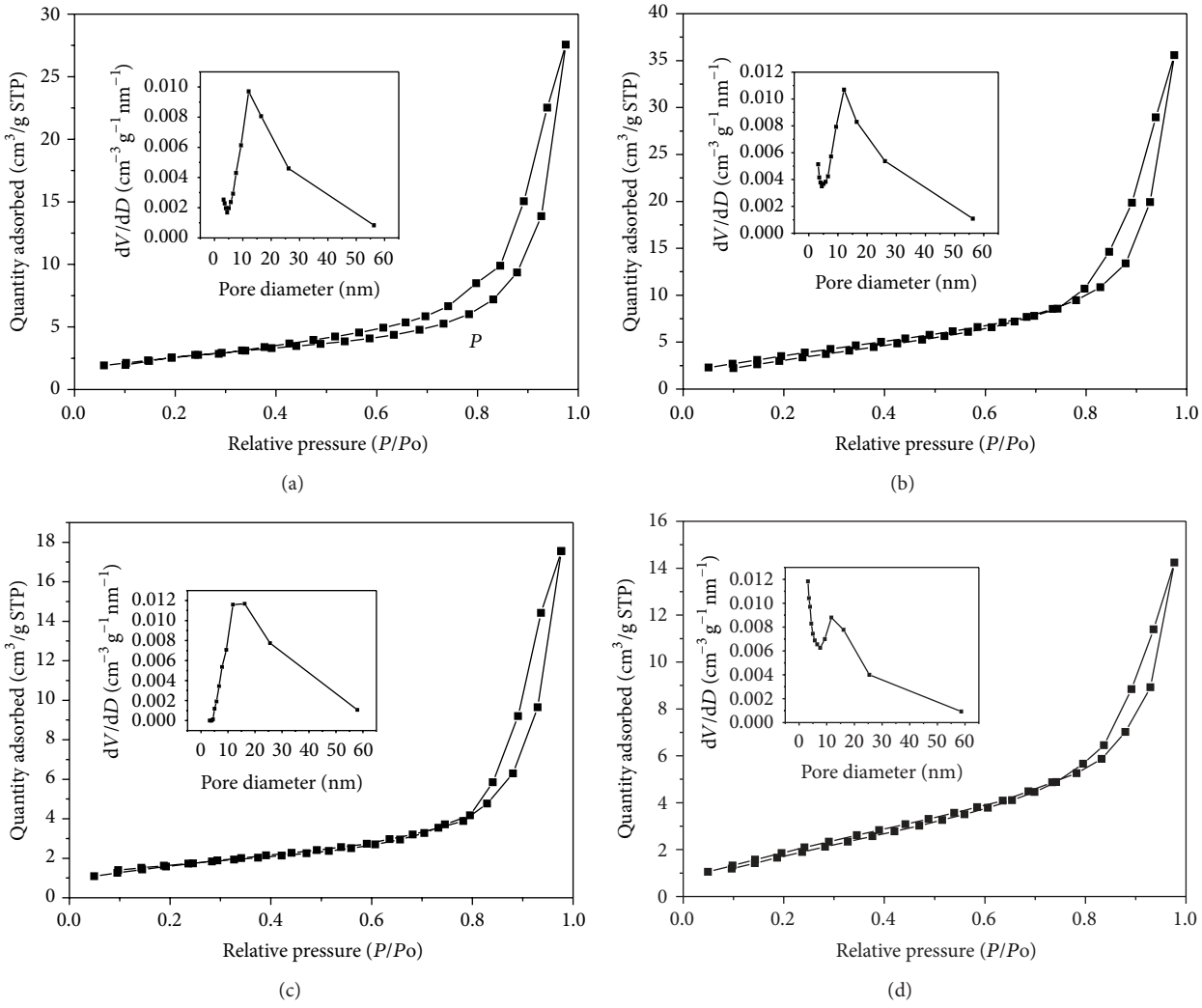

FIGURE 6: N_2 adsorption-desorption isotherms of as-prepared Co_3O_4 nanostructures at 77 K: (a) microrods, (b) spindle-like architectures, (c) nanorod bundles, and (d) nanorods. Inset in each isotherm is the corresponding pore size distributions.

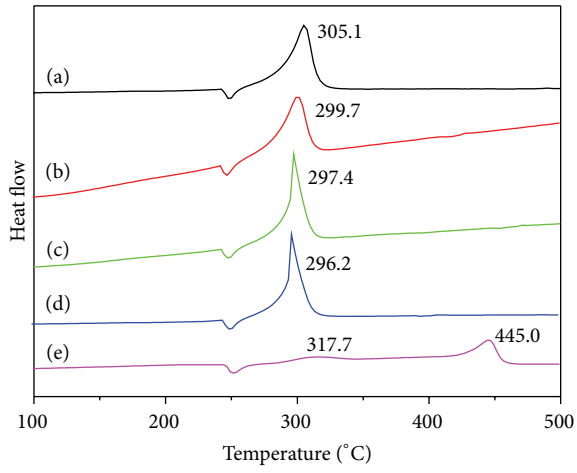

FIGURE 7: DSC curves of the AP samples after addition of various Co_3O_4 nanostructures: (a) 2 wt% Co_3O_4 microrods, (b) 2 wt% Co_3O_4 spindle-like architectures, (c) 2 wt% Co_3O_4 nanorod bundles, (d) 2 wt% Co_3O_4 nanorods, and (e) pure AP.

(no. BK20140013), Jiangsu Postdoctoral Science Foundation (no. 1401051C), and the Senior Intellectuals Fund of Jiangsu University (nos. 14JDG058 and 11JDG098).

References

[1] Q. Hua, T. Cao, X.-K. Gu et al., "Crystal-plane-controlled selectivity of Cu_2O catalysts in propylene oxidation with molecular oxygen," *Angewandte Chemie—International Edition*, vol. 53, no. 19, pp. 4856–4861, 2014.

[2] Y. Zhong, J. Wang, R. Zhang et al., "Morphology-controlled self-assembly and synthesis of photocatalytic nanocrystals," *Nano Letters*, vol. 14, no. 12, pp. 7175–7179, 2014.

[3] Y. Li and Y. Huang, "Morphology-controlled synthesis of platinum nanocrystals with specific peptides," *Advanced Materials*, vol. 22, no. 17, pp. 1921–1925, 2010.

[4] L. Chen, J. Hu, R. Richards, S. Prikhodko, and S. Kodambaka, "Synthesis and surface activity of single-crystalline Co_3O_4 (111) holey nanosheets," *Nanoscale*, vol. 2, no. 9, pp. 1657–1660, 2010.

[5] B. Yan, L. Chen, Y. Liu et al., "Co_3O_4 nanostructures with a high rate performance as anode materials for lithium-ion batteries, prepared via book-like cobalt-organic frameworks," *CrystEngComm*, vol. 16, no. 44, pp. 10227–10234, 2014.

[6] H. Wang, L. Zhang, X. Tan et al., "Supercapacitive properties of hydrothermally synthesized Co_3O_4 nanostructures," *The Journal of Physical Chemistry C*, vol. 115, no. 35, pp. 17599–17605, 2011.

[7] Y. Lü, W. Zhan, Y. He et al., "MOF-templated synthesis of porous Co_3O_4 concave nanocubes with high specific surface area and their gas sensing properties," *ACS Applied Materials and Interfaces*, vol. 6, no. 6, pp. 4186–4195, 2014.

[8] Y. Du, W. Huang, Z. Hua et al., "A facile ultrasonic process for the preparation of Co_3O_4 nanoflowers for room-temperature removal of low-concentration NO_x," *Catalysis Communications*, vol. 57, pp. 73–77, 2014.

[9] T. Zhu, J. S. Chen, and X. W. Lou, "Shape-controlled synthesis of porous Co_3O_4 nanostructures for application in supercapacitors," *Journal of Materials Chemistry*, vol. 20, no. 33, pp. 7015–7020, 2010.

[10] L. Hu, Q. Peng, and Y. Li, "Selective synthesis of Co_3O_4 nanocrystal with different shape and crystal plane effect on catalytic property for methane combustion," *Journal of the American Chemical Society*, vol. 130, no. 48, pp. 16136–16137, 2008.

[11] D. Wang, Q. Wang, and T. Wang, "Morphology-controllable synthesis of cobalt oxalates and their conversion to mesoporous Co_3O_4 nanostructures for application in supercapacitors," *Inorganic Chemistry*, vol. 50, no. 14, pp. 6482–6492, 2011.

[12] L.-N. Jin, Q. Liu, and W.-Y. Sun, "Shape-controlled synthesis of Co_3O_4 nanostructures derived from coordination polymer precursors and their application to the thermal decomposition of ammonium perchlorate," *CrystEngComm*, vol. 14, no. 22, pp. 7721–7726, 2012.

[13] S. Chaturvedi and P. N. Dave, "A review on the use of nanometals as catalysts for the thermal decomposition of ammonium perchlorate," *Journal of Saudi Chemical Society*, vol. 17, no. 2, pp. 135–149, 2013.

[14] W. Wang and J. Yao, "Catalytic activity of magnetite with different shapes for the thermal decomposition of ammonium perchlorate," *Chemistry Letters*, vol. 43, no. 10, pp. 1554–1556, 2014.

[15] L.-N. Jin, Q. Liu, and W.-Y. Sun, "Room temperature solution-phase synthesis of flower-like nanostructures of $[Ni_3(BTC)_2{\cdot}12H_2O]$ and their conversion to porous NiO," *Chinese Chemical Letters*, vol. 24, no. 8, pp. 663–667, 2013.

[16] S. Jamil, M. R. Janjua, and T. Ahmad, "The synthesis of flower shaped microstructures of Co_3O_4 by solvothermal approach and investigation of its catalytic activity," *Solid State Sciences*, vol. 36, pp. 73–79, 2014.

[17] X. Guan, G. Li, L. Zhou, L. Li, and X. Qiu, "Template-free approach to core-shell-structured Co_3O_4 microspheres," *Chemistry Letters*, vol. 38, no. 3, pp. 280–281, 2009.

[18] E. Alizadeh-Gheshlaghi, B. Shaabani, A. Khodayari, Y. Azizian-Kalandaragh, and R. Rahimi, "Investigation of the catalytic activity of nano-sized CuO, Co_3O_4 and $CuCo_2O_4$ powders on thermal decomposition of ammonium perchlorate," *Powder Technology*, vol. 217, pp. 330–339, 2012.

[19] H. Zhou, B. Lv, D. Wu, and Y. Xu, "Synthesis and properties of octahedral Co_3O_4 single-crystalline nanoparticles enclosed by (111) facets," *CrystEngComm*, vol. 15, no. 41, pp. 8337–8344, 2013.

[20] X. Guan, L. Li, J. Zheng, and G. Li, "$MgAl_2O_4$ nanoparticles: a new low-density additive for accelerating thermal decomposition of ammonium perchlorate," *RSC Advances*, vol. 1, no. 9, pp. 1808–1814, 2011.

[21] X.-J. Shen, J.-P. Yang, Y. Liu, Y.-S. Luo, and S.-Y. Fu, "Facile surfactant-free synthesis of monodisperse Ni particles via a simple solvothermal method and their superior catalytic effect on thermal decomposition of ammonium perchlorate," *New Journal of Chemistry*, vol. 35, no. 7, pp. 1403–1409, 2011.